Assessment of Aged Transgenic Mice for Evidence of Amyloid Related Imaging Abnormalities of the Edema/Effusion Type

James A Goodman[1], Gary B Freeman[2], William Angus[2], Thomas P Brown[3], Peter Cheng-te Chou[1], and Kelly R Bales[4]

[1]*Pharmatherapeutics Precision Medicine Preclinical Imaging, Pfizer Worldwide Research and Development, Groton, CT, United States,* [2]*General Toxicology, Pfizer Worldwide Research and Development, Groton, CT, United States,* [3]*Investigative Pathology, Pfizer Worldwide Research and Development, Groton, CT, United States,* [4]*Neuroscience Research Unit, Pfizer Worldwide Research and Development, Groton, CT, United States*

Introduction: An increased incidence of MRI abnormalities referred to as vasogenic edema (VE) and microhemorrhage (mH) has been reported in Alzheimer's disease subjects treated with therapies targeting Aβ (1,2). The underlying mechanism(s) of these abnormalities are unknown, leading to the more general term of Amyloid Related Imaging Abnormalities of the Edematous/Effusive type (ARIA-E) or Hemorrhagic type (ARIA-H)(3). Observation of ARIAs in animal models would be an important step in elucidating the pathophysiological basis of these findings and understanding their relationship to therapies that target Aβ removal. Herein, we describe the spontaneous appearance of ARIA-E and -H in very old transgenic mice (APP+PS1) that represent a well characterized animal model of AD-like neuropathology.

Methods: All animal handling procedures were approved by the local Institutional Animal Care and Use Committee. This study used 18 APP+PS1 mice (19-23 months of age) that overexpress the amyloid precursor protein (APP) gene containing the Swedish mutation ($APP^{K670N,M671L}$;Tg2576) along with a presenilin mutation (PSEN1 M146L;PSAPP), five Tg2576 ($APP^{K670N,M671L}$;Tg2576) mice, and five HCHWA-Dutch mice. Animals were anesthetized with isoflurane and placed on an animal tray equipped with ear bars and a tooth bar for restraint. Anesthesia was delivered *via* a nose cone that was under a gentle vacuum to scavenge exhaled gases. Respiration rate and body temperature were monitored and maintained at physiologically normal levels. ***MR imaging***: A 1.5-cm actively-decoupled quadrature surface coil (Bruker, Entlingham, GR) was placed over the animal's head for signal reception and a 7.2-cm actively decoupled linear volume coil was used for transmission. 3D T2-weighted RARE images were acquired (TR=2.6 s, TE(eff)=100 ms, ETL=16, MTX=128 x 128 x 64, res=125 x 125 x 300 um^3) for ARIA-E detection. ARIA-H-sensitive scans were acquired using a 2D multislice Multi-Gradient Echo image (TR=3.0 s, TEs=3.5 + n*4.5, for n=0 – 11, res=125 x 125 x 500 um^3, slices=38). Following an interim analysis, a second cohort of ten APP+PS1 mice were evaluated. ***Image analysis:*** Two readers independently examined the T2-weighted images for ARIA-E, and the T2*-weighted images for ARIA-H. The variably T2*-weighted images were summed over the gradient echo train to improve the sensitivity to hemosiderin deposits while minimizing large scale image distortions. ***Histologic verification:*** Selected animals were taken for histological identification of their MR-visible lesions. MR images were used to guide the tissue sectioning. To visualize ARIA-E, brain sections were stained using an anti-albumin antibody (4). To visualize ARIA-H, replicate brain sections were stained with Perls' iron stain.

Results: ***ARIA-E:*** Two independent readers examined the T2-weighted images for lateralized hyperintense regions that were taken to be evidence of ARIA-E. No ARIA-E was observed in the Tg2576 or Dutch mice. Some extent of ARIA-E was observed in 20/28 APP+PS1 mice by observers 1 and 2. Of these 20 animals, ARIA-E was especially prominent in 8. Several patterns of ARIA-E were noted. The first pattern appeared as a perivascular ring of hyperintensity surrounding a vessel (Figure 1a). A second and more common pattern was observed in the ventral regions of the piriform cortical lobe and the medial nucleus of the amygdala (Figure 1b). This second pattern of ARIA-E was somewhat larger and more diffuse than the first pattern. In a single animal, we observed a thalamic hyperintensity that fit neither pattern and may have been related to mineralization (a common background finding in animals of this advanced age). Histological results showed albumin in the parenchyma in the anatomical region which had an MR-visible ARIA-E lesion (Figure 2). ***ARIA-H:*** Hemosiderin deposits in the parenchyma following microhemorrhage resulted in small, punctate hypointensities on T2*-weighted images (Figure 1c). Accurate identification of such hypointensities was challenging because partial volume effects and their proximity to regions of high magnetic susceptibility gradients may result in false negatives. Detection sensitivity was improved by summing over the train of 12 echoes, as described above. AIRA-H was observed in 0/5 Dutch mice, 0/5 Tg2576, and 21/28 APP+PS1 mice. These were primarily in the dorsal half of the cortex, but several appeared in the cerebellum. Hypointensities in the thalamus were not interpreted to be ARIA-H because age-related mineralization occurs in this region. Perls' iron positive foci histologically colocalized with these MR-visible ARIA-H lesions (data not shown).

Discussion: Histological evidence indicates some degree of correspondence between regions of T2-weighted hyperintensity and leakage of albumin from the intravascular space. Variation in microscopic correspondence between T2-weighted hyperintensity and parenchymal albumin deposition would be expected, due to the dramatic differences in size and diffusivity of water and albumin. The presentation of ARIA-E in this cohort of aged Aβ-bearing transgenic mice varied from small, subtle lesions to large, diffuse lesions that covered a substantial fraction of the parenchyma (Figure 1). Given the phenotypic variability of ARIA-E, detection of these findings can be somewhat challenging. MR hyperintensities are believed to reflect localized increases in extracellular proteinaceous fluid that may vary over time in both severity and size as this fluid occurs and is resorbed. As a result of this probable chronologic variation, many of the more subtle instances of ARIA-E may be overlooked and result in under detection in cohorts of mice imaged at only one time point. Recent reports characterizing ARIA-E in subjects participating in clinical studies investigating various Aβ lowering therapies have documented a similar spectrum of ARIA-E phenotypes that vary over time (1,2). In summary, we have demonstrated MR imaging can detect spontaneously-occurring intensity alterations consistent with ARIA-E and AREA-H in aged Aβ-bearing transgenic mice, with the APP+PS1 strain appearing to be most sensitive. The pathogenesis of these findings and their relevance to MR clinical observations are being evaluated in ongoing studies with therapies targeting Aβ reduction.

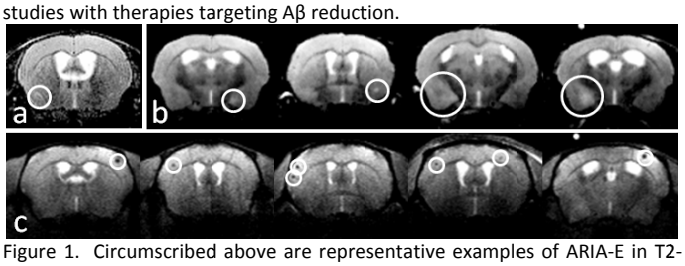

Figure 1. Circumscribed above are representative examples of ARIA-E in T2-weighted images (a-pervascular ring pattern, b-variable size/severity/diffuseness) and ARIA-H in T2*-weighted images (c). These images were chosen to exemplify various manifestations of the several patterns of abnormalities.

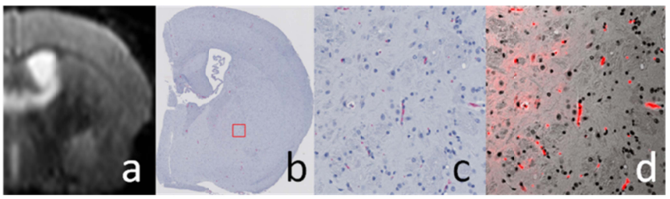

Figure. 2 Shown above are an *in vivo* T2-weighted image exhibiting a prominent ARIA-E lesion in the fundus of the striatum (a), a histologic section of the same brain using immunohistochemistry for albumin and a Vector red chromagen (b). When the area in the red box is magnified 50x, albumin is visible in capillary lumens but not in the parenchyma (c). When viewed under UV light, albumin becomes visible in both capillary lumens and in some adjacent parenchyma (d), consistent with an extravasation event at this site.

References: 1. Black, et al. *Alzh Dis Assoc Disord*. **24**:198-203 (2010). 2. Salloway, et al. *Neurology*. **73**:2061-70 (2009). 3. Sperling, et al. *Alzheimer's Dement*. **7**:367-85 (2011). 4. Zhu, et al. Exp Neurology. 169:72-82 (2001).